INTERNATIONAL JOURNAL FOR NUMERICAL METHODS IN FLUIDS
Int. J. Numer. Meth. Fluids **28**: 945–960 (1998)

ON SOME VARIATIONAL ACCELERATION TECHNIQUES AND RELATED METHODS FOR LOCAL REFINEMENT

RUNE TEIGLAND*

Department of Applied Mechanics and Engineering Sciences, University of California at San Diego, 9500 Gilman Drive, Mail Code 0411, La Jolla, California 92093-0411, USA

SUMMARY

This paper shows that the well-known variational acceleration method described by Wachspress (E. Wachspress, *Iterative Solution of Elliptic Systems and Applications to the Neutron Diffusion Equations of Reactor Physics*, Prentice-Hall, Englewood Cliffs, NJ, 1966) and later generalized to multilevels (known as the additive correction multigrid method (B.R Huthchinson and G.D. Raithby, *Numer. Heat Transf.*, **9**, 511–537 (1986))) is similar to the FAC method of McCormick and Thomas (S.F McCormick and J.W. Thomas, *Math. Comput.*, **46**, 439–456 (1986)) and related multilevel methods. The performance of the method is demonstrated for some simple model problems using local refinement and suggestions for improving the performance of the method are given. © 1998 John Wiley & Sons, Ltd.

KEY WORDS: variational acceleration method; composite grids; local refinement

1. INTRODUCTION

Many problems in the field of numerical partial differential equations exhibit solution behavior that requires more resolution in one area of the domain than in others. Many traditional techniques utilize a fine mesh covering the whole domain in order to resolve these fine local details. However, using a uniform global fine grid to resolve the local details often becomes too expensive, even for the largest computers. For these problems, some sort of local mesh refinement scheme becomes essential. Two different approaches, fixed local refinement and dynamic local refinement, are often distinguished. Dynamic and adaptive grid refinement used to follow moving fluid interfaces often requires complex data structures.

Fixed local grid refinement alone is used in this work. A typical example of a fixed localized phenomenon in reservoir simulation which requires special treatment is flow in the neighborhood of wells. Because of the rapidly changing behavior of the pressure in the vicinity of the wells, accurate pressure approximations require some type of local refinement. A regular local grid refinement scheme is used, in the sense that each grid cell in a certain subdomain is subdivided into a number of rectangular cells. Fixed and dynamic refinement techniques have been used in the reservoir context. Von Rosenberg used a finite difference refinement scheme based upon Taylor-series expansions for the constant coefficient problem [1]. Quandalle and Besset [2] discussed local refinement with local time stepping for reservoir applications.

* Correspondence to: Department of Applied Mechanics and Engineering Sciences, University of California at San Diego, 9500 Gilman Drive, Mail Code 0411, La Jolla, California 92093-0411, USA. E-mail: teigland@ames.ucsd.edu

CCC 0271–2091/98/160945–16$17.50

Received April 1997
Revised November 1997

Schmidt and Jacobs used a local refinement multigrid scheme to solve for an IMPES pressure equation [3]. Pedroza and Aziz [4] used a radial grid in local refinement around wells. Other examples of the use of local refinement schemes used in this context are given in References [5,6]. Most approaches used a global numbering of the nodes, which destroys the nice banded structure of regular grids. This paper describes an iterative technique that allows us, in some sense, to decouple the refined patches and the underlying global coarse grid; the coupling is through the internal boundary between coarse and refined regions. The technique used is a generalization of the well-known additive correction methods or variational acceleration techniques described in the book by Wachspress [7] and the additive correction method (ACM) in Reference [8]. The description of the method in conjunction with local refinement was proposed by Fladmark [9] and is similar to the fast adaptive composite grid (FAC) procedure of McCormick and Thomas [10].

In the context of uniform grids, the method was shown to be identical to a cell-centered multigrid algorithm using both restriction and prolongation operators based on piecewise constant interpolation [11,12]. In a later paper by Gjesdal [13] the same connection between ACMs and cell-centered multigrid methods was shown. Careful treatment of the finite difference stars near composite grid interfaces is important [14,15,2]. For illustration purposes, the discretization is given for both for a regular uniform grid and a non-uniform composite grid arising from the use of a locally refined grid. The efficient solution of the composite grid problem using the variational acceleration technique proposed in Reference [9] is presented. The connection between the method used here and the well-known FAC method proposed by McCormick and Thomas [10] and other multilevel methods [16] is shown. Some issues related to the construction of coarse grid matrices with the ACM method [17] are also discussed.

Finally, numerical experiments involving a simple model problem where an analytical expression for the solution is available and simulations involving more realistic reservoir conditions are presented and suggestions for improvement of the method is given.

2. DISCRETIZATION OF A SIMPLE MODEL PROBLEM

The conservative discretization is now discussed using the simplified pressure equation as a model problem:

$$\nabla\cdot(\lambda\nabla P) = -Q_{\mathrm{T}} + \phi c_{\mathrm{T}}\frac{\partial P}{\partial t}. \tag{1}$$

This equation is a simplified version of the parabolic pressure equation that stems from an IMPES formulation widely used in reservoir simulation studies [18]. P denotes an average pressure, $c_{\mathrm{T}} = c_{\mathrm{o}}S_{\mathrm{o}} + c_{\mathrm{w}}S_{\mathrm{w}}$ where c_α ($\alpha = \mathrm{o}, \mathrm{w}$) is the compressibility term and Q_{T} denotes total source terms, $\lambda = \lambda_{\mathrm{o}} + \lambda_{\mathrm{w}}$ denotes total transmissibility terms. Furthermore,

$$\lambda_\alpha = \frac{K\cdot k_{\mathrm{r}\alpha}}{\mu_\alpha}, \quad \alpha = \mathrm{o}, \mathrm{w}, \tag{2}$$

where K is the absolute permeability, $k_{\mathrm{r}\alpha}$ is the relative permeability of phase α, and μ_α is the viscosity. The saturation S_α ($\alpha = \mathrm{o}, \mathrm{w}$) is the fraction of the space available for flow occupied by the oil or water phase, thus $S_{\mathrm{o}} + S_{\mathrm{w}} = 1$. In the following discussion, additional incompressibility is assumed, i.e. $c_{\mathrm{T}} = 0$. The starting point of the discretization is not the differential Equation (1) but the primary balance equation.

Integrating the equation over a finite volume $V \subset \Omega$ (area in 2D) gives

$$-\int_V \nabla\cdot(\lambda\nabla P)\,\mathrm{d}V = \int_V Q_\mathrm{T}\,\mathrm{d}V. \tag{3}$$

Applying Gauss' divergence theorem, the volume integral on the left-hand-side is transformed into a surface integral (line integral in 2D), yielding

$$-\int_\Gamma (\lambda\nabla P)\cdot\vec{n}\,\mathrm{d}\Gamma = \int_V Q_\mathrm{T}\,\mathrm{d}V, \tag{4}$$

where $\vec{n}$ is the outward unit normal defined on Γ. Each side represents a flow rate in mass per unit time, and the term $(\lambda\nabla P)\cdot\vec{n}$ represents a flux across Γ. The equation can thus be interpreted as a conservation law for the volume V, which states that the net flow rate across the surface Γ balances with the net flow rate from interior sources. Flux conservation is important because it is well-known that conservation can be critical to the computation of the correct solution for many problems [19].

2.1. Discretization at regular points

For the cell-centered grid depicted in Figure 2, the surfaces of the boundary control volumes coincide with the boundary of the computational domain, so that a Neumann boundary condition is easily incorporated into the equations and conservation for the entire domain is therefore assured. An additional advantage of cell-centered grids when using multigrid methods is that the boundary of the control volumes on the fine grid (or patch) coincide with those of the coarse grids. For each cell $e(x, y)$ in our computational region the problem has been transformed into one of computing fluxes leaving or entering each cell. For the compressible case, i.e. when $c_\mathrm{T} \neq 0$, the discretization of the time dependent terms consists of replacing those partial derivatives by finite differences.

Let

$$F_x = -\lambda\frac{\partial P}{\partial x}, \qquad F_y = -\lambda\frac{\partial P}{\partial y}, \tag{5}$$

denote the fluxes, in the x- and y-directions, respectively.

If $e(x, y)$ is the cell shown in Figure 1 then the surface (line-) integral can be written as

$$\int_\Gamma F\cdot\vec{n}\,\mathrm{d}\Gamma = \int_\mathrm{E} F_x\,\mathrm{d}\Gamma - \int_\mathrm{W} F_x\,\mathrm{d}\Gamma + \int_\mathrm{N} F_y\,\mathrm{d}\Gamma - \int_\mathrm{S} F_y\,\mathrm{d}\Gamma. \tag{6}$$

Since $\lambda > 0$, we can write

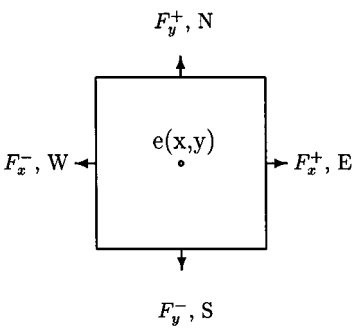

Figure 1. A grid cell; flux notation.

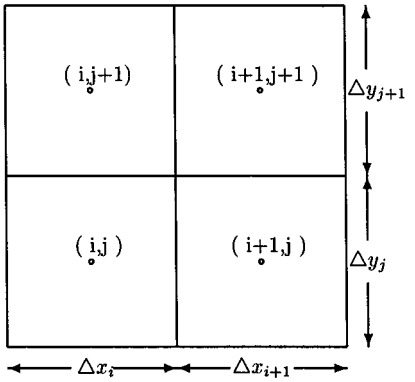

Figure 2. Cells with block sizes and numbering of points.

$$\frac{\partial P}{\partial x} = -\frac{F_x}{\lambda}.$$

Integrating along the segment $x_i \to x_{i+1}$ (see Figure 2),

$$P_{i+1,j} - P_{i,j} = -\int_{x_i}^{x_{i+1}} \frac{F_x^+(x, y_j)}{\lambda(x, y_j)}\,\mathrm{d}x. \tag{7}$$

Assuming that the flux does not vary much along the segment, the following approximation can be deduced for $F_x(x_i, y_j)$ at the east boundary:

$$P_{i+1,j} - P_{i,j} = -F_{x_{i+1/2,j}} \int_{x_i}^{x_{i+1}} \frac{\mathrm{d}x}{\lambda(x, y_j)}. \tag{8}$$

This gives

$$\int_{\mathrm{E}} F_x\,\mathrm{d}\Gamma = \Delta y F_{x_{i+1/2,j}} = -\frac{\Delta y}{\Delta x} \frac{P_{i+1,j} - P_{i,j}}{1/\Delta x \displaystyle\int_{x_i}^{x_{i+1}} (\mathrm{d}x/\lambda(x, y_j))}. \tag{9}$$

There are similar approximate relations for the other fluxes at the north, west and south boundaries of the cell. $\lambda_{i+1/2,j}$ is defined as

$$\lambda_{i+1/2,j} = \left(\frac{1}{\Delta x}\int_{x_i}^{x_{i+1}} \frac{\mathrm{d}x}{\lambda(x, y_j)}\right)^{-1}. \tag{10}$$

In the case where λ is constant within a cell, we obtain

$$\lambda_{i+1/2,j} = \frac{2\lambda_{i,j} \cdot \lambda_{i+1,j}}{(\lambda_{i,j} + \lambda_{i+1,j})}, \tag{11}$$

i.e. the usual harmonic average. If the same procedure is applied to all the line integrals in Equation (6), the discrete 'pressure' equation is obtained:

$$-\frac{\Delta y}{\Delta x}\lambda_{i+1/2,j}(P_{i+1,j} - P_{i,j}) - \frac{\Delta y}{\Delta x}\lambda_{i-1/2,j}(P_{i-1,j} - P_{ij}) - \frac{\Delta x}{\Delta y}\lambda_{i,j+1/2}(P_{i,j+1} - P_{i,j})$$
$$-\frac{\Delta x}{\Delta y}\lambda_{i,j-1/2}(P_{i,j-1} - P_{i,j}) = f_{i,j}, \tag{12}$$

where $f_{i,j}$ is the discrete form of the term

$$\int_V Q_T \, dV. \tag{13}$$

For the case of rectangular cells on a non-uniform mesh, the flux term $F_{x_{i+1/2,j}}$ is

$$F_{x_{i+1/2,j}} = -\frac{2\Delta y_j}{\Delta x_i + \Delta x_{i+1}} \lambda_{i+1/2,j}(P_{i+1,j} - P_{i,j}),$$

$$\lambda_{i+1/2,j} = \left(\frac{2}{\Delta x_i + \Delta x_{i+1}} \int_{x_i}^{x_{i+1}} \frac{dx}{\lambda(x, y_j)} \right)^{-1}.$$

Similarly, for the other flux terms this gives the case where λ is constant within a cell:

$$\lambda_{i+1/2,j} = \frac{2\lambda_{i,j} \cdot \lambda_{i+1,j}}{(\lambda_{i,j}\Delta x_{i+1} + \lambda_{i+1,j}\Delta x_i)} \Delta x_{i+1/2,j}, \tag{14}$$

where

$$\Delta x_{i+1/2,j} = \frac{1}{2}(\Delta x_i + \Delta x_{i+1}). \tag{15}$$

2.2. Discretization at irregular points

This section describes the conservative discretization in the case of a grid with locally refined patches. An example of a grid with locally refined patches is given in Figure 3. Consider the case of the irregular cell centered at (i_1, j_1) as shown in Figure 4. The two nodes marked x in this figure are fictitious points and are only used to facilitate the computation of the couplings across irregular interfaces. The approximation at the irregular points requires the finite difference scheme to conserve mass. This translates into a condition of conservation of fluxes. The case of Figure 4 requires that

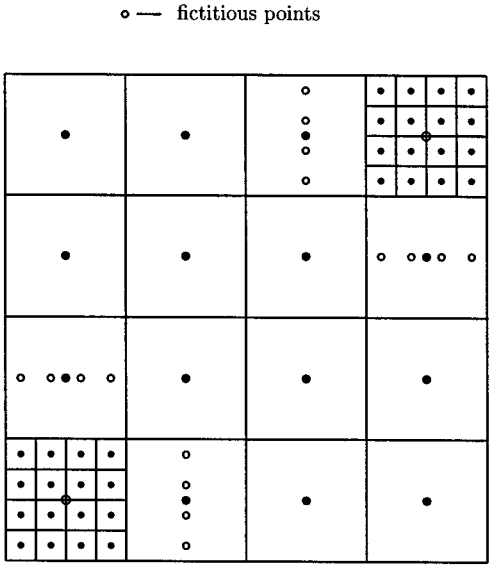

Figure 3. A composite grid.

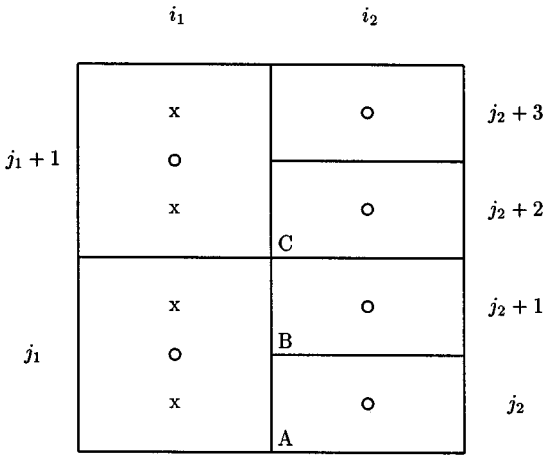

Figure 4. Finite difference cells near a local mesh boundary.

$$\int_{AC} F_x^+(x_i, y_j)\,d\Gamma = \int_{AB} F_x^-\,d\Gamma + \int_{BC} F_x^-\,d\Gamma. \tag{16}$$

For the first term on the right-hand-side of Equation (16) we have

$$\int_{AB} -\lambda \frac{\partial P}{\partial x}\,dy = \frac{\Delta y}{2}\frac{1}{\Delta x}\frac{P_{i_1,j_2} - P_{i_2,j_2}}{1/\Delta x \int_{x_{i_1}}^{x_{i_2}} dx/\lambda(x, y_{j_2})}. \tag{17}$$

Similarly,

$$\int_{BC} -\lambda \frac{\partial P}{\partial x}\,dy = \frac{\Delta y}{2}\frac{1}{\Delta x}\frac{P_{i_1,j_2+1} - P_{i_2,j_2+1}}{1/\Delta x \int_{x_{i_1}}^{x_{i_2}} dx/\lambda(x, y_{j_2+1})}. \tag{18}$$

In the case of constant interpolation considered here, it is assumed that the pressure at the fictitious points (i_1, j_2) and $(i_1,\ j_2+1)$ is the same as at (i_1, j_1), so that $P_{i_1,j_2} = P_{i_1,j_1}$ and $P_{i_1,j_2+1} = P_{i_1,j_1}$ in Equation (17). Note that for this simple approximation, the system of linear equations will remain symmetric if the system of linear equations corresponding to a regular grid itself is symmetric. The convergence properties of the finite difference system are quite poor. Ewing, *et al.* [14] showed that the rate of convergence in the discrete energy norm of this scheme is $\mathcal{O}(h^{1/2})$, h being the mesh size. A better approximation would be to use linear interpolation between coarse grid pressure values. For example the values of P at the fictitious points (i_1, j_2) and (i_1, j_2+1) are

$$P_{i_1,j_2+1} = \frac{1}{4}P_{i_1,j_1+1} + \frac{3}{4}P_{i_1,j_1}, \tag{19}$$

$$P_{i_1,j_2} = \frac{1}{4}P_{i_1,j_1-1} + \frac{3}{4}P_{i_1,j_1}. \tag{20}$$

Note that using linear interpolation as we do here gives rise to a non-symmetric matrix.

Forsyth and Sammon [5] showed that the approximation using constant interpolation lead to a truncation error $\mathcal{O}(h^{-1})$. However, in the discrete energy norm the difference scheme has $\mathcal{O}(h^{1/2})$ accuracy. For the case of linear interpolation the finite difference scheme has an

accuracy $\mathcal{O}(h^{3/2})$ [14]. The low order of convergence of the simplest difference scheme (case of constant interpolation), is due to its poor approximation properties at the irregular points.

In the fully implicit case the derivation of the equations at the irregular interfaces is completely analogous to the derivation above for the simple model problem (1). In computing the transmissibilities, both pressure and saturation must be evaluated at the new time level $n+1$, (since in the general case transmissibilities are functions of saturation and pressure). The discrete transmissibility across the regular face is given by

$$T_x^+(i,j) = \frac{\Delta y_j}{\Delta x_{i+1/2}} \left(\frac{k_r b}{\mu}\right)_{i+1/2,j} \cdot K_{i+1/2,j}, \tag{21}$$

where $K_{i+1/2,j}$ is given by an expression similar to Equation (11). Similarly,

$$T_y^+(i,j) = \frac{\Delta x_i}{\Delta y_{j+1/2}} \left(\frac{k_r b}{\mu}\right)_{i,j+1/2} \cdot K_{i,j+1/2}, \tag{22}$$

with similar expressions for $T_x^-(i,j)$ and $T_y^-(i,j)$. At the irregular face AC (see Figure 4) we have a similar formula to Equations (17) and (18) for the fluxes

$$\int_{AB} F_x^+ \, dy = (P_{i_1,j_2} - P_{i_2,j_2}) T_x^-(i_2,j_2), \tag{23}$$

$$\int_{BC} F_x^+ \, dy = (P_{i_1,j_2+1} - P_{i_2,j_2+1}) T_x^-(i_2,j_2+1), \tag{24}$$

where the transmissibilities now involves the use of the absolute permeability for irregular grids, as given by Equation (14). Therefore, in computing the terms $(k_r b/\mu)_{i+1/2,j}$, etc. it is useful to interpolate pressure and saturation to the fictitious points (i_1, j_2) and (i_1, j_2+1), so that the same routines can be used in these computations as for the regular interfaces.

3. EFFECTIVE SOLUTION OF THE COMPOSITE GRID EQUATIONS

Consider the composite grid problem

$$\mathcal{A}\vec{x} = \vec{y}. \tag{25}$$

$\mathcal{A}$ is the composite grid matrix and $\vec{x}$ and $\vec{y}$ are the composite grid solution and right-hand-side, respectively. We partition the nodes of the composite grid Ω into two disjoint sets, as in the previous section. Ω_F consists of those grid points in the refined region and Ω_C consists of the grid points in the non-refined region. $\tilde{\Omega}$ denotes the computational region when there is no refinement, i.e. a uniform coarse region. $\tilde{\Omega}$ is partitioned in an analogous manner. $\tilde{\Omega}_F$ contains the coarse grid points underlying the fine patch, and $\tilde{\Omega}_C = \Omega_C$. Partition the composite matrix $\mathcal{A}$ according to the partition of the domain:

$$\begin{bmatrix} \mathcal{A}_{CC} & \mathcal{A}_{CF} \\ \mathcal{A}_{FC} & \mathcal{A}_{FF} \end{bmatrix} \begin{bmatrix} \vec{x}_c \\ \vec{x}_f \end{bmatrix} = \begin{bmatrix} \vec{y}_c \\ \vec{y}_f \end{bmatrix}, \tag{26}$$

where $\vec{x}_c$ denotes the composite solution in the coarse region, dim N_c and $\vec{x}_f$ denotes the composite solution in the refined region, dim N_f. A similar partition for the matrix corresponding to $\tilde{\Omega}$, is

$$\begin{bmatrix} \tilde{A}_{CC} & \tilde{A}_{CF} \\ \tilde{A}_{FC} & \tilde{A}_{FF} \end{bmatrix} \begin{bmatrix} \tilde{\vec{x}}_c \\ \tilde{\vec{x}}_f \end{bmatrix} = \begin{bmatrix} \tilde{\vec{y}}_c \\ \tilde{\vec{y}}_f \end{bmatrix}. \tag{27}$$

The number of added coarse nodes that are now underlying the fine patch is N_{fc}. An algorithm is presented for solving the composite grid problem (26) that was proposed by Fladmark [9], defining

$$\tilde{N} = N_{\mathrm{c}} + N_{\mathrm{fc}}.$$

Let

$$\mathscr{M}_{\tilde{i}} = \{\text{fine cells within coarse cell number } \tilde{i}\}, \quad \tilde{i} = 1, 2, \ldots, \tilde{N}.$$

$\vec{\Psi}_{\tilde{i}}$ denotes a vector of order $N = N_{\mathrm{f}} + N_{\mathrm{c}}$ consisting of only zero-elements, except for unit elements at all $i \in \mathscr{M}_{\tilde{i}}$, $(\tilde{i} = 1, 2, \ldots, \tilde{N})$. Let $\vec{x}(k)$ be the kth iterate of $\vec{x}$. Choose a test function:

$$\vec{z} = \sum_{\tilde{i}=1}^{\tilde{N}} \tilde{x}_{\tilde{i}} \cdot \vec{\Psi}_{\tilde{i}} + \vec{x}(k) = \begin{bmatrix} \vec{z}_{\mathrm{c}} \\ \vec{z}_{\mathrm{f}} \end{bmatrix}, \quad z \in \mathbf{R}^N, \tag{28}$$

where $\tilde{x}_{\tilde{i}}$ is the $\tilde{i}$th component of $\vec{\tilde{x}} \in \mathbf{R}^{\tilde{N}}$.

Using $\vec{z}$ as a test function in a Galerkin method, for each coarse cell $\tilde{j}$ the following equation should be satisfied:

$$\langle \vec{\Psi}_{\tilde{j}}, \mathscr{A}\vec{z} \rangle = \langle \vec{\Psi}_{\tilde{j}}, \vec{y} \rangle, \quad \tilde{j} = 1, 2, \ldots \tilde{N}, \tag{29}$$

or

$$\tilde{A}\vec{\tilde{x}} = \vec{\tilde{y}}, \tag{30}$$

where $\tilde{A} = (\tilde{a}_{\tilde{i},\tilde{j}})$ is given by

$$\tilde{a}_{\tilde{i},\tilde{j}} = \sum_{i \in \mathscr{M}_{\tilde{i}}} \sum_{j \in \mathscr{M}_{\tilde{j}}} a_{i,j}, \tag{31}$$

$$\tilde{y}_{\tilde{i}} = \sum_{i \in \mathscr{M}_{\tilde{i}}} \left(y_i - \sum_{j=1}^{N} a_{i,j} \cdot x_j(k) \right). \tag{32}$$

The solution to Equation (30) yields the value of the test function $\vec{z}$ from Equation (28).

We now choose

$$\vec{x}_{\mathrm{c}}(k+1) = \vec{z}_{\mathrm{c}}. \tag{33}$$

The $(k+1)$th iterate of $\vec{x}_{\mathrm{f}}$ is computed from

$$\mathscr{A}_{\mathrm{FF}}\vec{x}_{\mathrm{f}}(k+1) = -\mathscr{A}_{\mathrm{FC}}\vec{x}_{\mathrm{c}}(k+1) + \vec{y}_{\mathrm{f}}. \tag{34}$$

Therefore,

$$\vec{x}(k+1) = \begin{bmatrix} \vec{x}_{\mathrm{c}}(k+1) \\ \vec{x}_{\mathrm{f}}(k+1) \end{bmatrix}. \tag{35}$$

The iteration proceeds by returning to Equation (28).

This algorithm will now be described in a slightly different form and equivalence to the FAC procedure of McCormick and Thomas [10] is shown. Equation (28) is equivalent to

$$\vec{z} = \vec{x} + \mathbf{P}\vec{\tilde{x}}, \tag{36}$$

where $\mathbf{P}$ is a prolongation operator (constant interpolation with our choice of $\Psi_{\tilde{i}}$) that maps coarse grid functions in $\tilde{\Omega}$ to composite grid functions in Ω, i.e.

$$\mathbf{P} \cdot \vec{\tilde{x}} = \begin{bmatrix} \mathbf{I} \cdot \vec{\tilde{x}}_{\mathrm{C}} \\ \mathbf{P}_{\mathrm{C}}^{\mathrm{F}} \cdot \vec{\tilde{x}}_{\mathrm{F}} \end{bmatrix}. \tag{37}$$

Equation (29) is now equivalent to

$$\mathbf{R} \circ \mathscr{A} \cdot (\vec{x} + \mathbf{P} \cdot \tilde{\vec{x}}) = \mathbf{R} \cdot \vec{y}, \tag{38}$$

or

$$\mathbf{R} \circ \mathscr{A} \circ \mathbf{P} \cdot \tilde{\vec{x}} = \mathbf{R} \cdot \vec{y} - \mathbf{R} \circ \mathscr{A} \cdot \vec{x}, \tag{39}$$

where $\mathbf{R}$ is a restriction operator that maps composite grid functions in Ω to coarse grid functions in $\tilde{\Omega}$. Our coarse grid operator has been constructed using a procedure analogous to the Galerkin procedure described in Reference [20]. Defining the coarse grid operator as

$$\mathbf{A} = \mathbf{R} \circ \mathscr{A} \circ \mathbf{P}, \tag{40}$$

gives the coarse grid defect equation

$$\mathbf{A} \cdot \tilde{\vec{x}} = \mathbf{R} \circ (\vec{y} - \mathscr{A} \cdot \vec{x}). \tag{41}$$

The right-hand-side is the restriction of the composite grid residual to the coarse grid $\tilde{\Omega}$.

The algorithm can now be summarized in the following steps:

Algorithm 3.1

Step 1: Solve for $\tilde{\vec{x}}$ from Equation (41).

$$\tilde{\vec{x}} = \mathbf{A}^{-1}(\mathbf{R} \cdot (\vec{y} - \mathscr{A}\vec{x})).$$

Step 2: Having solved for $\tilde{\vec{x}}$, interpolate the correction to the composite grid and defect correct the composite solution $\vec{x}$, so that

$$\vec{z} = \vec{x} + \mathbf{P}\tilde{\vec{x}}.$$

Step 3: Solve the fine grid problem:

$$\mathscr{A}_{\mathrm{FF}}\vec{x}_{\mathrm{f}}(k+1) = -\mathscr{A}_{\mathrm{FC}}\vec{x}_{\mathrm{c}}(k+1) + \vec{y}_{\mathrm{f}}.$$

This completes one step of the algorithm.

The algorithm proceeds until the composite residuals have converged to some tolerance ϵ. In Step 1, the coarse grid is solved as if there were no fine patch. After the first cycle, the right-hand-side of Step 1 is the composite residual that makes a correction to the most recent approximation to the composite grid solution. Step 3 solves the fine patch using the previous approximation for the coarse and interface solution. This algorithm is completely analogous to the algorithm described by McCormick and Thomas in Reference [10], pp. 444. This is referred to as the two-level exact solver cycle of FAC. This implies that the 'corrections' from the underlying coarse patch are zero, since we are solving exactly on the refined regions as well as for the uniform coarse grid problem. The FAC algorithm attempts to solve the composite grid problem (25) by way of uniformly rectangular discrete equations. Information is passed through the internal boundary between coarse and refined regions. Therefore, the method can be seen as a domain decomposition method. FAC can be interpreted as a Schwarz-like domain decomposition method in terms of subdomains Ω_{F} and Ω_{C}. Solving in Step 1 and Step 3 is not restricted to using exact solvers. For the approximate FAC algorithm where e.g. a couple of steps of a suitable relaxation method are used, defect corrections from coarse grids underlying fine grid patches and restriction of residuals from patch to coarse grid are required. Liu [21] used a $V(2, 1)$ MG cycle as an approximate solver.

Note that the FAC procedure is 'relatively easy' to implement into existing simulators, because the existing highly efficient solvers can be used for the regular grids. Routines that

compute composite residuals, modify transmissibilities at irregular interfaces and interpolation routines are needed in order to patch the FAC algorithm into existing simulators.

Note that the band structure and corresponding efficiency are lost when the composite grid equations are solved explicitly for the ordering of given unknowns. The FAC method has the attribute that it is suitable for vectorization and adds important parallel capabilities. Note that the solution of the systems on the patches on the same level can be done on different processors.

4. A NOTE ON THE ACM METHOD FOR UNIFORM GRIDS

On uniform grids, the ACM method [17] and the Galerkin technique described in the previous section are equivalent when using both restriction and prolongation operators based on piecewise constant interpolation. In the context of the variational formulation, this corresponds to using a Galerkin approach where basis and test functions are equal. The Galerkin technique was first applied as an acceleration method by Wachspress in 1962 [7] for acceleration of the iterative solution of linear equations in nuclear reactor calculations.

Consider the linear system

$$A\vec{x} = \vec{y}. \tag{42}$$

Let $M_{\tilde{i}}$ denote the set of fine cells that are defined in the weighted sum for the restriction operation centered on coarse cell $\tilde{i}$.

Referring to Figure 5, the coarse grid cell (i, j) is made up by the 2×2 fine grid cells $(2i-1, 2j-1)$, $(2i, 2j-1)$, $(2i-1, 2j)$ and $(2i, 2j)$. Let $\vec{x}(k)$ denote the solution vector at iteration k. Following the same derivation as in Equations (28)–(32) the coarse grid system to solve is

$$\tilde{A}\vec{\tilde{x}} = \vec{\tilde{y}}, \tag{43}$$

or elementwise as

$$\tilde{a}_{\tilde{i},\tilde{j}} = \sum_{i \in \mathcal{M}_{\tilde{i}}} \sum_{j \in \mathcal{M}_{\tilde{j}}} a_{i,j}, \tag{44}$$

and

$$\tilde{y}_{\tilde{i}} = \sum_{i \in \mathcal{M}_{\tilde{i}}} r_i, \tag{45}$$

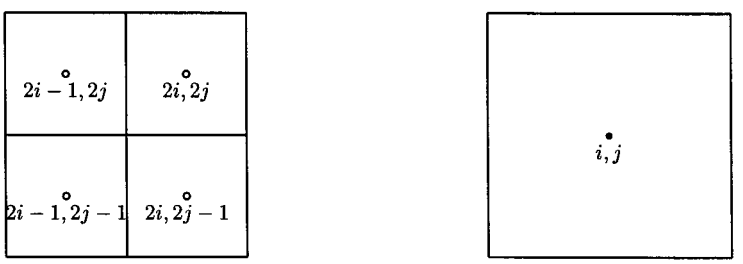

Figure 5. The subdivision of a coarse grid cell into four fine cells.

where r_i denotes the fine grid residual. Using the subdivision of cells as in Figure 5 it is straightforward to show the correspondence between the Galerkin approach and the ACM method of Hutchinson and Raithby, see e.g. Reference [12]. Conservation properties of the Galerkin approximation were shown in References [22,12]. In order to ensure multigrid convergence, i.e. for the rate of convergence to be independent of the grid size, the restriction and prolongation operators must satisfy the accuracy requirement:

$$m_{\mathrm{P}} + m_{\mathrm{R}} > M, \tag{46}$$

where M is the order of the differential operator and m_{P} and m_{R} are the order of the restriction and prolongation operator, respectively [23]. This requirement holds for elliptic operators, but the condition given by Equation (46) does not hold for non-elliptic and singular perturbation problems [24]. Yavneh [24] found that the corresponding conclusion for Galerkin coarsening is that non-elliptic operators require larger orders of the prolongation and restriction operators than the rule given by Equation (46).

Now, considering the usual discretization of the Laplace operator in one dimension, we have in stencil notation for the fine grid matrix (see e.g. Reference [20])

$$A_h[-1 \quad 2 \quad -1], \tag{47}$$

and

$$A_{2h} = \frac{1}{2} A_h, \tag{48}$$

using a direct discretization of the Laplace operator on the coarse grid (labeled $2h$). Using a low-order Galerkin approximation, as in the ACM method [17], gives

$$A_{2h} = A_h \tag{49}$$

(similar results applies to the two- and three-dimensional Laplace operator). Standard multigrid with a discretized coarse grid operator, linear prolongation and constant restriction yields grid-independent convergence rates for the Laplace operator [23,20]. Studying the ACM method and the coarse grid operator given by Equation (49) reveals that it is the same as the fine grid operator (no scaling). Unless we are solving for a problem with pure Neumann boundary conditions, the ACM method yields an error component of low-frequency on the fine grid. This will in turn deteriorate the convergence rate. In Reference [13] it was suggested that the ACM approach can offer improved convergence rates for diffusion dominated problems, by choosing a more accurate restriction and prolongation operator. This is not entirely correct, because the coarse grid operator must be consistent with a discretized operator on the coarse grid.

In Reference [13] it was stated that the 'FLUX' scheme of Ersland and Teigland [22] corresponds to a low-order Galerkin operator. This is not entirely correct. The 'FLUX' scheme corresponds to a consistently scaled low-order RAP operator (Galerkin) that treats diffusive fluxes correctly, and thus reconstructs the exact discretization on coarse grids. The method in Reference [22] is equivalent to the coarse grid operators presented in References [25,26].

5. NUMERICAL EXPERIMENTS FOR PROBLEMS WITH LOCAL REFINEMENT

In this section, some numerical computations for the model problem given below are presented. The convergence rates varying the ratio of coarse to fine grid, and the interpolation scheme are studied. The stopping criteria for the FAC iterations is given by

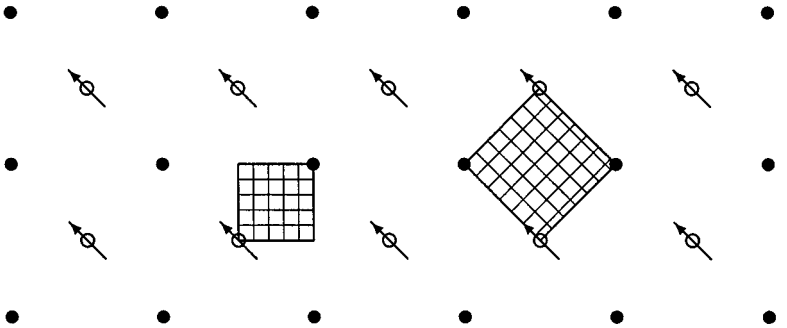

Figure 6. Repeated five-spot well pattern with diagonal and parallel grids.

$$r^T \cdot r < \epsilon, \tag{50}$$

where $\epsilon = 10^{-10}$ and r is the composite grid residual at the current iteration step. The average reduction factor reported is given by

$$\rho = \left(\frac{\Delta}{\Delta_0}\right)^{1/\text{iter}}, \tag{51}$$

where Δ_0 is the norm of the initial residual, Δ is the norm of the last residual, and iter is the number of iterations required to achieve the desired accuracy ϵ. In order to study the accuracy of the scheme the following error estimator is considered:

$$\epsilon_0 = \left\{ \sum_{(x,y)\in\Omega} h^2 (p(x, y) - \tilde{p}(x, y))^2 \right\}^{1/2},$$

where $p(x, y)$ and $\tilde{p}(x, y)$ denotes the exact solution and computed solution respectively.

5.1. Test case I

The problem considered here is the well-known repeated five-spot well pattern, see e.g. Reference [27] for a detailed description and derivation of the solution. In the quarter five-spot problem a square domain in the horizontal plane is considered, with injection and production wells at opposite corners along one of the diagonals (see Figure 6).

By summing up the contributions from an infinite pattern of injectors and producers of uniform strength, a solution of the Poisson equation is obtained away from the well locations:

$$p(x, y) = \frac{1}{4\pi} \sum_{m=-\infty}^{\infty} (-1)^{|m|} \ln \left\{ \frac{\cosh(\pi/2\,(x + y - 2m)) + \cos(\pi/2(x - y))}{\cosh(\pi/2(x + y - 2m)) - \cos(\pi/2(x - y))} \right\}. \tag{52}$$

In the reference system chosen, the producers are located at the points $(x = 2i + 1, y = 2j + 1)$ and the injectors at $(x = 2i, y = 2j)$, where $i, j \in \mathbf{Z}$. The factor $1/4\pi$ corresponds to sources of unit strength. Each term in the above sum represents the contributions from the wells along the line $x + y = 2m$, $m \in \mathbf{Z}$. The summation of Equation (52) must be performed numerically.

The solution obtained from Equation (52) can then be compared with numerical computations. For the diagonal grid of Figure 6, fluid of unit viscosity is injected into a reservoir of constant thickness and unit permeability with an injection well at (0, 0) and a production well at (1, 1). Note that the two different grids of Figure 6 provide the possibility to check the discretization for grid orientation effects. Severe grid orientation effects occur with the conventional five-point cell-centered grid. The computational region is $\Omega = [0,\ 1]^2$.

The diagonal grid of Figure 6 was used and rectangular refinement was introduced in the vicinity of each well, i.e. in the lower left and upper right corner of Ω. The areas to be refined were fixed so that the total rectangularly refined domain is

$$\Omega_{\mathrm{RW}} = [0, 1/4]^2 + [3/4, 1]^2. \tag{53}$$

For the purpose of studying accuracy and convergence on the refined patches, consider the modified domain

$$\Omega_{\mathrm{RW}_{\mathrm{mod}}} = \Omega_{\mathrm{RW}} = [0, 1/8]^2 - [7/8, 1]^2, \tag{54}$$

i.e. excluding a fixed area around the singularities (wells).

In test case I (Table I) there was an increase in the error for fixed h_c and for increased ratio of h_c/h_f. Similar results were reported in Reference [14] for a slightly different problem. An approximation to the composite residual was used in computing the right-hand-side of the coarse grid problem in Step 1 of the FAC algorithm. Injection is used to restrict the composite residual to the coarse grid and constant interpolation is used in computing the composite grid residual. There are several methods for improving the accuracy results: more careful treatment of the composite residuals and use of multilevel local refinement, keeping the ratio of coarse-to-fine levels small.

5.2. Test case II

In this test problem we solve for the pressure equation (1). The computational region is again $\Omega = [0, 1]^2$ and the refined region is Ω_{RW} as defined above in Equation (53). Water is injected in the lower left corner of Ω, i.e. at $(0, 0)$, and oil is produced in the upper right corner, i.e. at $(1, 1)$.

The capillary pressure $P_c(S_w)$ is taken to be zero, and the rock porosity $\phi = 0.2$, (porosity is a measure of the pore space and hence the fluid capacity of the medium). The pressures P_o and P_w, o and w denoting oil and water respectively, in any two phases at any point in the porous medium, are assumed to be related to each other via the capillary pressure P_c, see, e.g. Reference [27] for a discussion of these concepts. The oil and water viscosities are 1.0

Table I. Accuracy results for test case I: constant interpolation

H_c	h_c/h_f	ϵ_0	N
1/8	1	2.0–3	64
1/8	2	9.2–4	88
1/8	4	1.1–3	184
1/8	8	1.1–3	568
1/16	1	3.4–4	256
1/16	2	2.7–4	352
1/16	4	2.9–4	736
1/16	8	2.9–4	2104
1/32	1	1.2–4	1024
1/32	2	7.2–5	1408
1/32	4	7.4–5	2944
1/32	8	7.5–5	9088

Table II. Relative permeabilities for water and oil as functions of water saturation

S_w	Relative permeability	
	k_{r_w}	k_{r_o}
0.200	0.000	0.3380
0.265	0.002	0.2464
0.330	0.008	0.1730
0.395	0.018	0.1159
0.460	0.032	0.0730
0.525	0.050	0.0422
0.590	0.080	0.0216
0.655	0.098	0.0091
0.720	0.128	0.0027
0.785	0.162	0.0003
0.850	0.200	0.0000

and 0.31 cp, respectively. The time steps where initially 0.1 days, and water injection rates at 244 ft^3 day^{-1}; production rates are the same. The oil compressibility was fixed at 1.47×10^{-5} psi^{-1} and water compressibility was set to zero. The saturation dependent values shown in Table II (relative permeabilities as functions of water saturation) are used in the simulations.

Homogeneous permeability values, $K_x = 100$ mD and $K_y = 100$ mD are used. The average reduction factors as defined in Equation (51) are tabulated, where ρ_0 is the result of using the simplest interpolation operator in Step 2 of algorithm, and ρ_1 is the result of using linear interpolation. Slightly better convergence rates are obtained using linear interpolation versus constant interpolation. The extra computational effort involved in using linear interpolation is only marginal compared with the use of the constant interpolation method as described in Section 2.2. The exact analytical solution to test case II is not known, therefore, iterative convergence rates are included in Table III (based on residuals, see Equation (51)). The use of linear interpolation is more accurate than using constant interpolation at fictitious points, as shown in Reference [15].

Table III. Iterative convergence rates for test case II

h_c	h_c/h_f	ρ_1	ρ_0	N
1/8	2	6.7–3	1.0–2	88
1/8	4	1.1–2	2.6–2	184
1/8	8	1.8–2	4.1–2	568
1/16	2	9.3–3	1.1–2	352
1/16	4	8.6–3	2.6–2	736
1/16	8	1.2–2	4.2–2	2104
1/32	2	9.7–3	1.1–2	1408
1/32	4	1.1–2	2.6–2	2944
1/32	8	1.7–2	4.2–2	9088

6. CONCLUSIONS

The use of a local refinement scheme based upon a variational acceleration technique proposed in Reference [9] was investigated. It was shown that the scheme is equivalent to the FAC method of McCormick and Thomas [10]. The scheme is also equivalent to the ACM method [17] on uniform grids. The scheme was applied to some simple problems where a fixed refined patch was put around wells. The results obtained showed that the scheme can be effective when higher resolution is needed in some areas more than others, such as around wells in numerical reservoir simulation. In order to fully utilize the potential of the scheme in e.g. numerical reservoir simulation, multilevel refinement must be employed. Although the numerical examples presented here are taken from numerical reservoir simulation, the techniques presented in this paper apply equally to different problems.

ACKNOWLEDGMENTS

This work was partially supported by the Research Council of Norway through grant number 75482/410.

REFERENCES

1. D.U. von Rosenberg, 'Local grid refinement for finite difference methods', in *Proc. 57th Annual Fall Technical Conference*, *Paper SPE 10974*, New Orleans, 1982.
2. P. Quandalle and P. Besset, 'Reduction of grid effects due to local sub-gridding in simulations using a composite grid', *in Proc. of the SPE 1985 Reservoir Simulation Symposium*, *Paper SPE 13527*, Dallas, February 1985.
3. G.H. Schmidt and F.J. Jacobs, 'Adaptive local grid refinement and multi-grid in numerical reservoir simulation', *J. Comput. Phys.*, **77**, 140–165 (1988).
4. O.A. Pedrosa and K. Aziz, 'Use of hybrid grid in reservoir simulation', in *Proc. SPE 1985 Middle East Technical Conference*, *SPE 13507*, Bahrain, 1985.
5. P.A. Forsyth and P.H. Sammon, 'Local mesh refinement and modeling of faults and pinchouts', in *Proc. SPE 1985 Reservoir Simulation Symposium*, *Paper SPE 13524*, Dallas, February 1985.
6. M.L. Wasserman, 'Local grid refinement for three-dimensional simulators', in *Proc. 9th SPE Symp. on Reservoir Simulation*, *Paper SPE 16013*, San Antonio, February 1987.
7. E. Wachspress, *Iterative Solution of Elliptic Systems and Applications to the Neutron Diffusion Equations of Reactor Physics*, Prentice-Hall international series in applied mathematics, Prentice-Hall, Englewood Cliffs, NJ, 1966.
8. A. Settari and K. Aziz, 'A generalization of the additive correction methods for the iterative solution of matrix equations', *SIAM J. Numer. Anal.*, **10**, 506–521 (1973).
9. G.E. Fladmark, 'A numerical method for local refinement of grid blocks applied to reservoir simulation', Paper presented at the Gordon Research Conference for Modeling of Flow in Permeable Media at Andover, USA, August 9–13, 1982.
10. S.F. McCormick and J.W. Thomas, 'The fast adaptive composite grid (FAC) method for elliptic equations', *Math. Comput.*, **46**, 439–456, (1986).
11. R. Teigland and G.E. Fladmark, 'Cell-centered multigrid methods in porous media flow', in *Multigrid Methods III*, *Vol. 98 of Int. Series of Numerical Mathematics*, Birkhauser, Basel, 1991, pp. 365–376.
12. R. Teigland, 'On multilevel methods for numerical reservoir simulation', *Ph.D. dissertation*, University of Bergen, Department of Mathematics, *Report no. 92*, *ISSN 0084-778x*, July 1991.
13. T. Gjesdal, 'A note on the additive correction multigrid method', *Int. Comm. Heat Mass Trans.*, **23**, 293–298 (1996).
14. R.E. Ewing, R.D. Lazarov and P.S. Vassilevski, 'Local refinement techniques for elliptic problems on cell-centered grids', *EORI 1988-16*, University of Wyoming, 1988.
15. R.E. Ewing, R.D. Lazarov and P.S. Vassilevski, 'Local refinement techniques for elliptic problems on cell-centered grids I: Error analysis', *Math. Comput.*, **56**, 437–461 (1991).
16. B. Smith, P. Bjørstad and W. Gropp, *Domain Decomposition*, *Parallel Multilevel Methods for Elliptic Partial Differential Equations*', Cambridge University Press, Cambridge, 1996.
17. B.R. Hutchinson and G.D. Raithby, 'A multigrid method based on the additive correction strategy', *Numer. Heat Trans.*, **9**, 511–537 (1986).
18. D.W. Peaceman, *Fundamentals of Numerical Reservoir Simulation*, Elsevier, Oxford, 1977.

19. J.W. Thomas, *Numerical Partial Differential Equations*, *Finite Difference Methods*, Vol. 22 of Texts in Applied Mathematics, Springer, New York, 1995.
20. P. Wesseling, *An Introduction to Multigrid Methods*, Wiley, Chichester, 1992.
21. C. Liu, 'The finite volume element (fve) method and fast adaptive composite grid method (fac) for the incompressible Navier–Stokes equations', in *Proc. 4th Copper Mountain Conf. on multigrid methods*, 1989.
22. B.G. Ersland and R. Teigland, 'Comparison of two cell-centered multigrid schemes for problems with discontinuous coefficients', *Numer. Meth. PDE*, **9**, 265–283 (1993).
23. W. Hackbusch, *Multigrid Methods and Applications*, Vol. 4, Springer Series in Computational Mathematics, Springer, Berlin, 1985.
24. I. Yavneh, 'Coarse-grid correction for nonelliptic and singular perturbation problems', (unpublished) in *MGNET* (http://casper.cs.yale.edu/mgnet/www/ mgnet-papers.html).
25. M. Khalil and P. Wesseling, 'Vertex-centered and cell-centered multigrid for interface problems', *J. Comput. Phys.*, **98**, 1–10 (1992).
26. J. Molenaar, 'A simple cell-centered multigrid method for 3d interface problems', *Comput. Math. Appl.*, 31, 25–33 (1996).
27. M. Muskat, *The Flow of Homogeneous Fluids through Porous Media*, International series in physics, McGraw-Hill, New York, 1937.

